JOC Article

Nitrogen Inversion in Cyclic Amines and the Bicyclic Effect

Anatoly M. Belostotskii,* Hugo E. Gottlieb, and Michael Shokhen*

Chemistry Department, Bar-Ilan University, Ramat-Gan 52900, Israel

belostot@mail.biu.ac.il; shokhem@mail.biu.ac.il

Received April 1, 2002

The hitherto unsolved problem of the origin of the unusually high nitrogen inversion−rotation (NIR) barriers in 7-azabicyclo[2.2.1]heptanes (the bicyclic effect) was examined using the natural bond orbital (NBO) approach. Reinvestigating the NIR barrier for tropane by DNMR, we found that NIR barriers increase smoothly on going from nitrogen-bridged bicyclic systems of a larger ring size to the smaller ring homologous systems. The experimental NIR barriers are reproduced with good accuracy using the MP2/6-31G* level of theory. The NBO analysis for these and other azabicycles led to the conclusion that the height of these barriers is mostly determined by the energy of the σ-orbitals of the $C_{\alpha-}C_{\beta}$ bonds as well as the nitrogen lone pair. Thus, the bicyclic effect is actually an extreme case of a common *$C_{\alpha-}N-C_{\alpha}$ tripyramid geometry−NIR barrier* dependence for N-bridged bicyclic amines. By establishing the rate-determining role of the *$C_{\alpha-}N-C_{\alpha}$ tripyramid* fragment for NIR, we have derived the first sufficiently accurate quantitative correlations *amine geometry−NIR barrier* for monocyclic as well as bicyclic *N*-H and *N*-Me amines (i.e., for an amine set which also includes the bicyclic effect systems).

1. Introduction

Abnormally high barriers for nitrogen inversion (actually for nitrogen inversion−C−N rotation, NIR[1a−c]) in azanorbornanes **1** (Figure 1) were for the first time described by Lehn as the bicyclic effect.[2] Since this observation, many investigations were undertaken to reveal structural features causing this conformational dynamic effect (for a short critical overview see ref 3a as well as the Results and Discussion), but no comprehensive explanation was actually proposed. Remarkably, studies[3a,4] which deal especially with the origin of the bicyclic effect have concluded that the barrier increase cannot be satisfactorily explained within the limits of classical models (i.e., in terms of steric interactions or ring strain) and that an orbital model should be invoked. Our study[3a] of amines **1** bearing homologous exocyclic N-substituents indicated that the slowing of the NIR process among these compounds may be explained as derived from strain. However, this concept was unable to explain the striking barrier difference of 5−6 kcal/mol between azabicycloheptane **1a** and the close bicyclic analogues of larger ring size, e.g., azabicycles **2a** and **3a** (Figure 1). Only in crowded systems (e.g., *N*-*t*-Bu compound **1b**; Figure 1) are steric interactions sufficiently strong to be considered as a crucial factor. The measured "usual" NIR value for **1b** originates from the trivial destabilization of the stable amine conformation[3b] caused by the flattening of the N-containing fragment.[3a] Careful attempts[4] to find an *azacycle structure−NIR barrier* relationship for a representative set of monocyclic and bicyclic amines (obviously, including analogues **1a**, **2a**, and **3a**) led Nelsen and co-workers to a heuristic notion: such a relationship is insufficient for understanding the bicyclic effect since it has an orbital nature,[4] instead.

Also, later studies[5a,6] do not display structural factors which increase NIR barriers in azanorbornanes **1**. It was suggested that the bicyclic effect should be inherent also to other nitrogen-bridged bicycles for which at least one azetidine cycle is the ring component of their backbone.[5a] Another study[6] gave new examples of 7-azabicycloheptanes **1** possessing sterically hindered amino fragments and therefore relatively low NIR barriers due to the

(1) (a) Bushweller, C. H.; Anderson, W. G.; Stevenson, P. E.; Burkey, D. L.; O'Neil, J. W. *J. Am. Chem. Soc.* **1974**, *96*, 3892−3900. (b) Bushweller, C. H. In *Acyclic Organonitrogen Stereodynamics*; Lambert, J. B., Takeuchi, E., Eds.; VCH Publishers: New York, 1992; pp 1−55. (c) Belostotskii, A. M.; Aped, P.; Hassner, A. *J. Mol. Struct.: THEOCHEM* **1997**, *398*−*399*, 427−434.

(2) Lehn, J. M. *Fortschr. Chem. Forsch.* **1970**, *15*, 311−377.

(3) (a) Belostotskii, A. M.; Gottlieb, H. E.; Hassner, A. *J. Am. Chem. Soc.* **1996**, *118*, 7783−7789. (b) Lambert, J. B. *Top. Stereochem.* **1971**, *6*, 19−105. (c) Calculated ΔE values should in principle represent an enthalpy-near energy. Nevertheless, the comparison herein is with the measured $\Delta G^{\ddagger}$ and not $\Delta H^{\ddagger}$ values because NMR line shape analysis provides the values of $\Delta G^{\ddagger}$ quite accurately while $\Delta H^{\ddagger}$ values are usually determined with substantially bigger experimental error. On the other hand, we assume that calculated ΔE values represent the $\Delta G^{\ddagger}$ values satisfactorily since the entropy contribution is relatively small for these amines (see, e.g., the NMR data for **2a** in section 2.1). In addition, the conformational distribution increment into Gibbs energy is actually absent for these rigid bicyclic systems. (d) The B3LYP/6-31G*-provided barriers of NIR for azacycles **1a** and **3a** are 10.0 and 5.7 kcal/mol, respectively (i.e., 1.5−3.5 kcal/mol of NIR barrier underestimation).

(4) Nelsen, S. F.; Ippoliti, J. T.; Frigo, T. B.; Petillo, P. A. *J. Am. Chem. Soc.* **1989**, *111*, 1776−1781.

(5) (a) Belostotskii, A. M.; Aped, P.; Hassner, A. *J. Mol. Struct.: THEOCHEM* **1998,** *429*, 265−273. (b) Belostotskii, A. M.; Gottlieb, H. E.; Aped, P.; Hassner, A. *Chem.−Eur. J.* **1999**, *5*, 449−455. (c) Anet, F. A. L. In: Rabideau, P. W. *Conformational Analysis of Cyclohexenes, Cyclohexadienes and Related Hydroaromatic Compounds*; VCH Publishers: New York, 1989; pp 3−45.

(6) Malpass, J. R.; Butler, D. N.; Johnston, M. R.; Hammond, M. L. A.; Warrener, R. N. *Org. Lett.* **2000**, *2*, 725−728.

10.1021/jo020221i CCC: $22.00
Published on Web 11/27/2002

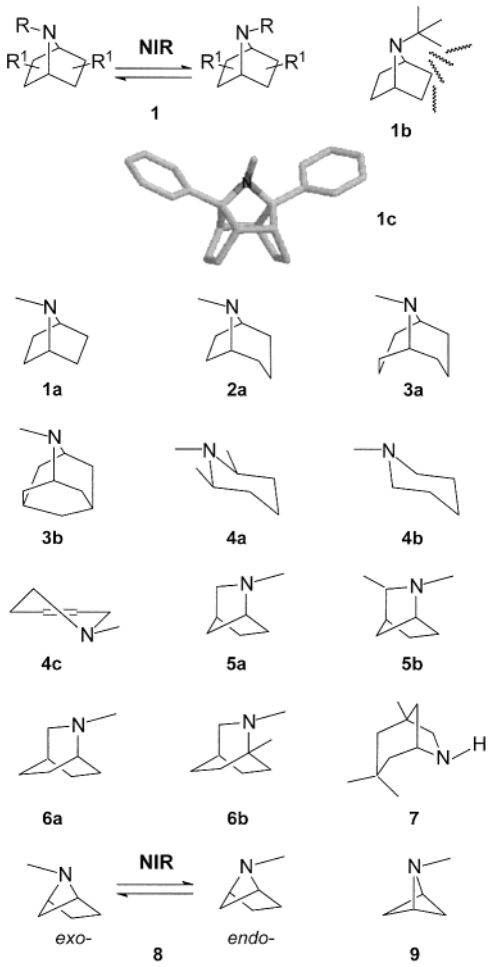

FIGURE 1. Amines **1a**−**c** to **9**. NIR is shown for the examples of azabicycles **1** and **8**. The stable conformer of **1b** is significantly destabilized by repulsive steric interactions (shown by wavy lines) between the *exo*-protons of the bicyclic backbone and the *N*-*t*-Bu substituent (ref 3a). The lowest energy conformers are shown for 1,4-diphenylazanorbornane **1c** (the RHF/6-31G*-optimized geometry is presented without hydrogens) as well as for **3a**, **4a**−**c**, and **5a,b** (*endo*-conformers), **6a,b** (*endo*-conformers), and **7**.

above-mentioned flattening of the nitrogen pyramid in the stable conformation.

In this study, we approach the problem of the bicyclic effect origin using natural bond orbital (NBO) analysis.[7a−c] This method has been successfully employed for the description of the role of separate structural fragments, e.g., in the conformational equilibrium of alkylamines.[7d] 7-Azabicycloalkanes **1a**, **2a**, and **3a** were chosen as closely related model compounds of increasing ring size. We intended to identify localized NBOs which are responsible for the NIR barrier diversity in these compounds and thus to identify molecular fragment(s) of explicit significance for NIR. Other amine analogues, monoazacycles **4a**−**c** and 2-azabicycloalkanes **5a,b**, **6a,b**, and **7** (Figure 1), were selected to examine whether a quantitative azacycle structure−NIR barrier relationship exists for mono- and polycyclic amines.

2. Results and Discussion

2.1. NMR Studies. It is accepted that azanorbornane **1a** belongs to the bicyclic effect systems,[4] while pseudopelletierine **3a** and 2-azaadamantane **3b** do not[4,8a] (see Table 1 for the experimental values of the free energy of activation for NIR, $\Delta G^{\ddagger}$). The measured NIR barrier for tropane **2a** (9.2 kcal/mol[8b]) is substantially lower than the NIR barrier for **1a** but slightly higher than that for **3a**. Therefore, compound **2a** was considered[3a,4,5] as not belonging to the bicyclic effect systems, and the statement that this effect appears straight away in small-size azabicycles (i.e., possessing four- or five-membered ring components) is still current.

We reinvestigated the NIR barrier for bicycle **2a** and measured it for monocycle **4c** in a CD_2Cl_2 solution by means of line shape analysis of the temperature-dependent ^{13}C and ^{1}H NMR spectra (the barriers for **1a** and **3a,b** were measured[4,8a] by the same DNMR techniques in CD_2Cl_2 for **1a**[4] and in a mixture of Me_2CO-d_6−CF_2Cl_2 for **3a,b**[8a]). It was found that for **2a** the $\Delta G^{\ddagger}$ of NIR is 11.1 ± 0.1 kcal/mol in the temperature range 210−230 K and that it is temperature-independent in this interval. We can conclude that the NIR barriers increase smoothly with a decrease of ring size in the azabicycles (see Table 1). In the sequence *lower barrier*−*higher barrier*, the NIR barrier for azabicyclooctane **2a** (a compound with one pyrrolidine ring) lies midway between a usual (6−8 kcal/mol) NIR barrier value (azabicyclononane **3a**, a compound without pyrrolidine rings) and a high NIR barrier value (azabicycloheptane **1a**, a compound with two pyrrolidine rings). The presence of a five-membered ring as a component of a rigid nitrogen-bridged bicyclic skeleton provides a significant (∼3 kcal/mol per ring) increase of the NIR barrier. This gradual barrier change obviously indicates the presence of a smooth *azacycle geometry*−*NIR barrier* relationship.

The signals of the geminal ring protons of piperideine **4c** (this compound was taken into consideration as one of the model cyclic amines for the establishment of the azacycle structure−NIR barrier relationship; see section 2.4) undergo broadening and then splitting as the temperature is lowered. The measured barrier for the corresponding conformational dynamic process is 8.8 ± 0.1 kcal/mol at 154.0 and 174.5 K and 8.9 ± 0.1 kcal/mol at 185.1 K. In general, it is problematic to assign observed temperature-induced changes in piperidine derivatives to a certain intramolecular motion, and additional studies are necessary.[5b] In the case of **4c**,[8c] however, we can conclude a priori that this barrier corresponds to NIR since the six-membered ring flattening caused by the endocyclic double bond leads to a significant decrease of the barriers of ring inversion (RI).[5c] For instance, the

(7) (a) Reed, A. E.; Curtiss, L. A.; Weinhold, F. *Chem. Rev.* **1988**, *88*, 899−926. (b) Carpenter, J. E.; Weinhold, F. *J. Am. Chem. Soc.* **1988**, *110*, 368−372. (c) Foster, J. P.; Weinhold, F. *J. Am. Chem. Soc.* **1980**, *102*, 7211−7218. (d) Taurian, O. E.; Contreras, R. H. *J. Mol Struct.: THEOCHEM* **2000**, *504*, 119−126.

(8) (a) Nelsen, S. F.; Weisman, G. R.; Clennan, E. L.; Peacock, V. E. *J. Am. Chem. Soc.* **1976**, *98*, 6893−6896. (b) Schneider, H.-J.; Sturm, L. *Angew. Chem.* **1976**, *88*, 574−575. (c) Gilchrist, J.; Goderin, H. *Chem. Phys.* **1983**, *79*, 307−320. (c) Also in the case of *N*-methyl-1,2,3,4-tetrahydroisoquinoline, the measured barrier (8.4 kcal/mol) was assigned to NIR (Davis, M.; Hugel, M. H.; Lakhan, R.; Ternai, B. *Aust. J. Chem.* **1976**, *29*, 1445−1458). (d) Anet, F. A. L.; Yavari, I.; Ferguson, I. J.; Katritzky, A. R.; Moreno-Manas, M.; Robinson, M. J. T. *Chem. Commun.* **1976**, 399.

TABLE 1. Calculated (MP2/6-31G*, kcal/mol) and Experimental (by DNMR, kcal/mol) NIR Barriers, Averaged Bond Angles α_{av} and β_{av} (deg; for Stable Conformers) at the N and C_α Atoms, Respectively, Occupancy of the Nitrogen Lone Pair Orbital, and sp-Character of This Orbital[a] (%) for the Stable Conformers of Azabicycles 1a, 2a, 3a,b, 4a,c, 5a,b, 6a, and 7

entry	calcd ΔE	DNMR $\Delta G^{\ddagger}$ (ref)	α_{av}	β_{av}	occupancy	s	p
1a	13.1	13.8 (4)	108.5	104.6	1.92565	17.91	82.03
exo-**2a**	10.5[b]	11.1[b] (this work)	108.5	108.2	1.92878	17.61	82.32
endo-**2a**	9.1[c]	10.0[c] (this work)	112.1	108.2	1.91635	14.24	85.71
3a	8.0	7.1 (8a)	112.3	111.7	1.91891	13.96	85.99
3b		7.8 (8a)	113.6	109.8	1.92009	14.10	85.85
4a	10.2		110.7	110.2	1.91706	15.80	84.15
4c	9.3[c]	8.9[c] (this work)					
exo-**5a**	6.5[d]	6.9 (13a)	109.8	104.1	1.92992	16.32	83.19
endo-**5a**	6.8[e]	7.2 (13a)	112.1	104.4	1.91673	13.73	86.22
5b	7.9		112.2	107.0			
6a	6.4	6.6 (13a)	111.9	108.6	1.91597	14.19	87.76
6b		6.6 (8a)	112.0	109.0			
7		4.9 (8c)	108.1	108.5			

[a] The rest is related to the d-hybridization. [b] Half-barrier for the *exo-N*-Me → *endo-N*-Me conformational transition. [c] Half-barrier for the *endo-N*-Me → *exo-N*-Me conformational transition (the values of $\Delta G°$ for the *exo-N*-Me → *endo-N*-Me and *N*-Me_{eq} → *N*-Me_{ax} conformational equilibrium in **2a** and **4c**, respectively, were measured by us previously[21a]). [d] Half-barrier for the *exo-N*-Me → *endo-N*-Me conformational transition. [e] Half-barrier for the *endo-N*-Me → *exo-N*-Me conformational transition.

experimental RI barrier for cyclohexene is only 5.3 kcal/mol.[5c] The calculated barrier (see below) for NIR in amine **4c** is 9.3 kcal/mol. Since our ab initio calculations provide sufficiently reliable values for NIR barriers, we view this very good correspondence between the experimental and calculated values (see Table 1) as a solid confirmation of our assignment of the barrier to NIR and not to RI. Of course, we cannot exclude the possibility that a concerted dynamic process of RI and NIR (RINIR) possesses the same rate as NIR and thus the temperature-induced changes in ^{1}H NMR spectra of **4c** result from both NIR and RINIR.

As we lower the temperature below ~180 K (at which point the ring protons have decoalesced), the widths of the signals of the carbons of **4c** start to increase. The broadening varies from carbon to carbon (up to ca. 3 Hz at 174.5 K, 5 Hz at 154.0 K), while some signals remain sharp. The only plausible cause for such a pattern is the onset of freezing of the conformational equilibrium with a certain population of a minor species (e.g., see ref 8d); increased solution viscosity tends to evenly widen all NMR signals in the molecule. A reasonable explanation in this case (see Figure 2) is that RI is interconverting conformers with equatorial and axial *N*-Me substituents.

2.2. NIR Barrier Calculations. Barriers of NIR for *N*-Me amines **1a**, **2a**, **3a**, **4a,c**, **5a,b**, **6a**, **8**, and **9** were calculated at the MP2/6-31G* level (using the Gaussian98 package[9]). MM3-derived structures were used as starting geometries for the ab initio energy minimization for the stable conformers as well as the transition states (see refs 3a and 10 for the MM3-based methodology of generation of NIR transition states). These geometries were subsequently optimized at the RHF/3-21G, at the RHF/6-31G*, and finally at the B3LYP/6-31G* (for compounds **1a** and **3a**) or MP2/6-31G* (for compounds **1a**, **2a**, **3a**, **4a,c**, **5a,b**, **6a**, **8**, and **9**) level of theory.

The experimental $\Delta G^{\ddagger}$ value and the difference between full electron energies (not corrected to the zero-point energy) of the NIR transition state and the corresponding stable conformer (ΔE) were compared for each

(9) Gaussian98, Gaussian Inc., Pittsburgh, PA, 1998.

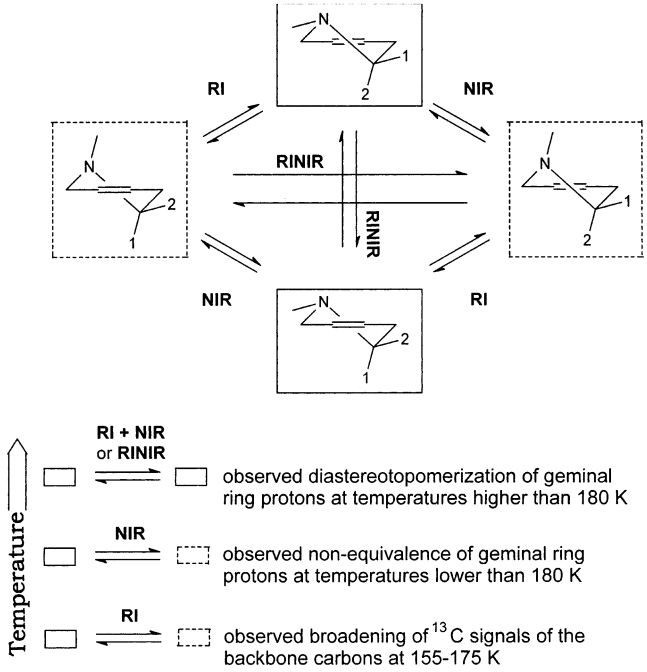

FIGURE 2. Conformational dynamics and its effects on temperature-variable NMR spectra of piperideine **4c**. Minimal energy and higher energy conformers of **4c** are shown in rectangles and in dotted rectangles, respectively. Diastereotopomerization of geminal ring protons is illustrated for the example of the *equatorial*−*axial* positional exchange of the 6-H protons (depicted by numbers 1 and 2).

amine **1a**, **2a**, and **3a**.[3c] For the first time calculations provide representative values for the NIR barriers for the bicyclic effect systems. In contrast to a poor estimate by MM3[3a] and AM1[4] of the NIR barriers for the bicyclic effect systems **1**, the results provided by MP2/6-31G* are in good accordance with the experimental $\Delta G^{\ddagger}$ values for **1a**, **2a**, and **3a** (as well as for other amines, **5a** and **6a**; Table 1).[3d] The difference between the experimental and MP2/6-31G* values for the barriers is less than 0.9 kcal/mol. Linear regression analysis for these results at the MP2/6-31G* level demonstrated sufficiently good cor-

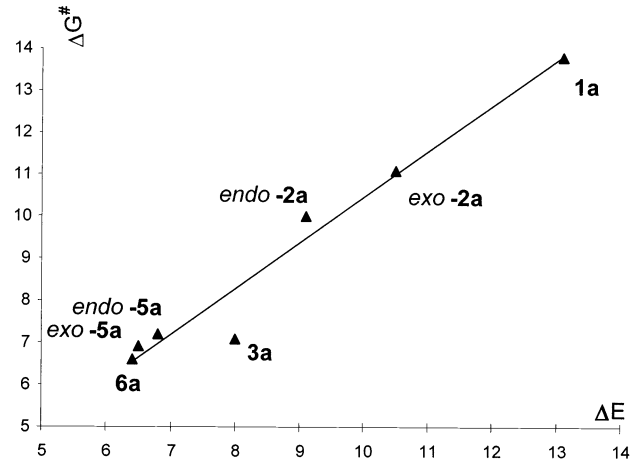

FIGURE 3. Linear regression analysis for the calculated barriers (MP2/6-31G*-provided values, kcal/mol) and the experimental NIR barriers (kcal/mol) for azabicycles **1a**, **2a**, **3a**, **5a**, and **6a**.

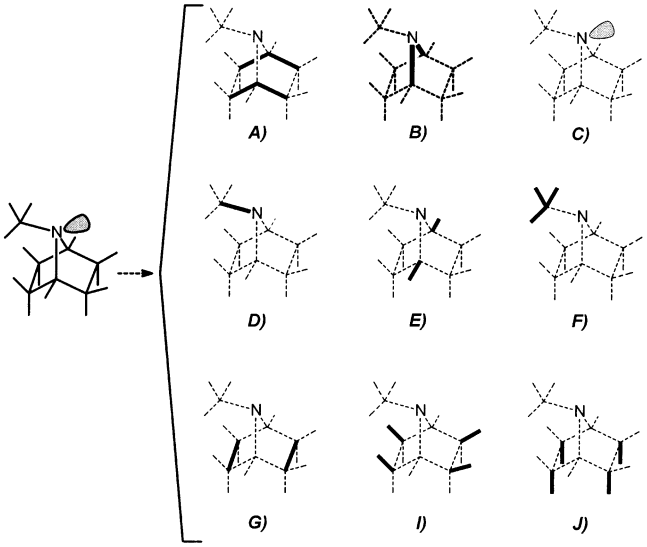

FIGURE 4. Formal marking out of azabicycle **1a** into fragments A−J (in bold or in gray; the remaining structure is shown by dotted lines).

relation between the calculated and measured barrier values (R^2 = 0.961 and the standard error is 0.6 kcal/mol at the 98% level of confidence; Figure 3). Thus, the accuracy of our calculations is sufficiently high to provide a reliable quantitative analysis of the trend for the orbital effects in the bicyclic amines considered. The obtained results also confirm the observed gradual increase of NIR barriers (see the above NMR-related discussion) parallel to the decrease of the size of the ring components of the bicyclic skeleton.

2.3. Identification of Structural Fragments Which Determine the NIR Rate. Methodology. Approaching the molecular structure of bicycles **1a**, **2a**, and **3a** as a set of nonoverlapping fragments F_1, ..., F_n, which are common for these compounds (e.g., C−N and C_α–C_β bonds, the nitrogen lone pair; see Figure 4), it is in principle possible to identify molecular domains which determine the above-mentioned azacycle geometry−NIR barrier relationship. To locate these domains, an NBO analysis[7a−c] (implemented into the Gaussian98 package[9]) has been performed for the stable conformers of **1a**, **2a**, and **3a** as well as for the corresponding NIR transition states at the MP2/6-31G* level of theory. This consideration permits the energy contributions of separate structural fragments F_k to the corresponding NIR barriers to be revealed and thus their relative significance, e.g., for the NIR kinetics, to be analyzed.

The NIR barrier $E(\mathbf{j})$ for amine **j** may be represented as a difference between its electron energy $E(\mathbf{j}_{TS})$ for the NIR transition state and the electron energy $E(\mathbf{j}_{SC})$ for the corresponding stable conformer (eq 1a).[3c] Indexes TS and SC denote the amine NIR transition state and the related stable conformer.

$$E(\mathbf{j}) = E(\mathbf{j}_{TS}) - E(\mathbf{j}_{SC}) \qquad (1a)$$

$E(\mathbf{j})$ may be represented as the sum of the energy contributions $E_k(\mathbf{j})$ of fragments F_k to the NIR barrier of this amine (see eq 2a).

$$E(\mathbf{j}) = \sum_k^N E_k(\mathbf{j}) \qquad (2a)$$

Within the limits of the NBO approach, each fragment F_k of amines **1a**, **2a**, and **3a** may be considered as an assembly of M elementary structural units (bond and lone pair NBOs inherent to F_k). Therefore, electron energy E_k of fragment F_k may be partitioned into energies E_i^{L} of occupied NBOs and energies E_i^{DA} of donor−acceptor interactions of these NBOs with vacant NBOs (eq 3a).

$$E_k = \sum_i^M E_i^{\,L} + \sum_i^M E_i^{\,DA} \qquad (3a)$$

In the present analysis of the origin of the bicyclic effect, we consider the change $\Delta E(\mathbf{j})$ of the NIR barrier for amine **j** relative to the NIR barrier for amine **1a** (eq 4a) as a trend in the NIR barrier change for amino structures **1a**, *exo*-**2a**, *endo*-**2a**, and **3a** (**j** = **1a**, *exo*-**2a**, *endo*-**2a**, and **3a**). In other words, for these amines the $\Delta E(\mathbf{j})$ value shows an NIR barrier decrease for amine **j** relative to **1a**. Obviously, the contribution $\Delta E_k(\mathbf{j})$ of each fragment F_k in this barrier change $\Delta E(\mathbf{j})$ (see eqs 2a and 5a) serves to reflect the role of fragments F_1, ..., F_n in the NIR barrier trend for this amine series.

$$\Delta E(\mathbf{j}) = E(\mathbf{1a}) - E(\mathbf{j}) \qquad (4a)$$

$$\Delta E_k(\mathbf{j}) = \sum_i^M \Delta E_i^{\,L}(\mathbf{j}) + \sum_i^M \Delta E_i^{\,DA}(\mathbf{j}) \qquad (5a)$$

We divided up the structures of amines **1a**, **2a**, and **3a** into fragments A (the C_α–C_β bonds), B (the endocyclic C_α–N bonds), C (the nitrogen lone pair), D (the exocyclic C_α–N bond), E (the bridgehead C−H bonds), F (the C−H bonds of the *N*-Me group), G (the C_β–C_β and C_β–C_γ bonds), I (the *exo*-C_β–H bonds), and J (the *endo*-C_β–H bonds; see the example of amine **1a** in Figure 4). The importance of the relative orientation of C_α–C_β bonds (i.e., an equivalent of fragment A in the N-bridged bicyclic amines) for the kinetics of NIR in alkylamines was demonstrated for the example of 2,2-disubstituted aziri-

dines.[11a] Also fragment E, fragments B + C + D (i.e., the N-pyramid), and fragments F + I were discussed in the literature[3a,4,6,12,13a,c,14a,15] as NIR rate influencing.

To single out structural fragments F_k which provide the major energy contributions ΔE_k(**j**) to the barrier decrease ΔE(**j**), we employed the original methodology for analysis of *structure−trend* relationships proposed by Shokhen.[11b−d] This general approach is aimed at identification of the trend-determining set (TDS) of factors, which causes structural reorganization of molecular systems in a *certain* direction. According to this conve-

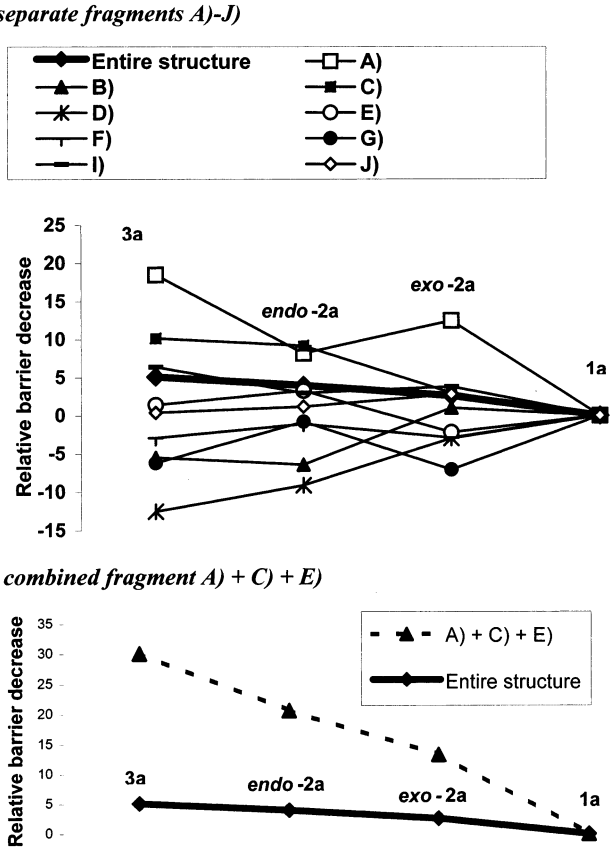

FIGURE 5. (ii) Trends of the NBO energy contributions ΔE_k-(**j**) of fragments A−J to the decrease of NIR barriers for amino structures **1a**, *exo*-**2a**, *endo*-**2a**, and **3a** (kcal/mol; shown as the NIR barrier decrease relative to amine **1a**). The bold line represents the trend of the decrease (relative to **1a**; kcal/mol) of the calculated NIR barriers for these amines. (ii) Trend of TDS contributions ΔE_{ACE}(**j**) (kcal/mol) for the **j** amines **1a**, *exo*-**2a**, *endo*-**2a**, and **3a** to the NIR barrier decrease relative to **1a** (the dotted line) and the trend of the decrease of the calculated barriers (kcal/mol) for these amines relative to **1a** (bold line).

nient methodology, TDS (i.e., the structural fragments to be identified) for the NIR barrier trend for amino structures **1a**, *exo*-**2a**, *endo*-**2a**, and **3a** is described by eq 1 (for justification see eq 4b from ref 11d), where ΔE_{TDS}(**j**) is the energy contribution of TDS in the total barrier decrease ΔE(**j**).

$$\Delta E_{TDS}(\mathbf{j})/\Delta E(\mathbf{j}) > 1 \qquad (1)$$

In other words, the fragments, which determine the observed barrier trend, should satisfy two clear criteria: (i) the same trend direction takes place for TDS and the entire structure, and (ii) the trend is maximally manifested for TDS (obviously stronger than for the entire structure).

TDS for Amines 1a, 2a, and 3a. We compared the trend of ΔE_k(**j**) for selected fragments among A−J as well as their combinations vs the trend of the decrease of the calculated NIR barriers ΔE(**j**) for azacycles **1a**, *exo*-**2a**, *endo*-**2a**, and **3a** (see Figure 5).[15] As expected, fragments A−J have different influences on the observed barrier decrease ΔE(**j**). Applying the condition from eq 1, we have localized the combined fragments A + C + E as perfectly

(10) Belostotskii, A. M.; Hassner, A. *J. Phys. Org. Chem.* **1999**, *12*, 659−663.

(11) (a) Shokhen, M. A.; Eremeev, A. V.; Kostyanovskii, R. G. *Izv. Akad. Nauk SSSR, Ser. Khim.* **1988**, 1942. (b) Shokhen, M. A.; Tikhomirov, D. A.; Eremeev, A. V. *Zh. Org. Khim.* **1984**, *20*, 2042−2052. (c) Shokhen, M. A.; Eremeev, A. V.; Kostyanovskii, R. G. *Izv. Akad. Nauk SSSR, Ser. Khim.* **1985**, 347−351. (d) A short description of this approach is presented below. Studying various molecular transformations (e.g., chemical reactions or conformational transitions), one usually considers a trend in a series $\{S_i\}_1^N$ of N molecules S_i subjected to a certain transformation. To study a trend, it is convenient to consider a series $\{\Delta E_i\}_1^{N-1}$ of $N-1$ relative transformation energies

$$\Delta E_i\colon \Delta E_i = E_i - E_o \qquad i = 1, ..., N-1 \qquad (1b)$$

where E_i and E_o are the transformation energies of molecule i and molecule o, accepted as a reference species, respectively. Actually any S_i molecule can be considered as a set of noninteracting structural elements s_k. Therefore, the ΔE_i value can be represented as a sum of Δe_k energy contributions from the corresponding structural elements s_k:

$$\Delta E_i = \sum_1^M \Delta e_k \qquad (2b)$$

where M is the total number of structural elements in molecule S_i. For chemical systems the trend of their chemical behavior is often their most interesting feature. Obviously, the exploration of a quantitative *structure−energy* relationship is an important tool in the analysis of the trend of different molecular transformations. Then, in terms of structural analysis (see eqs 1b and 2b), to understand the nature of the driving force for a certain change of a system state, one needs to analyze the influence of each structural element s_k on the value of ΔE_i. It is postulated that in a series $\{S_i\}_1^N$ of molecules subjected to the same kind of structural transformations caused by chemical reactions or conformational changes there is a TDS which is common for each S_i molecule. In energy terms, TDS has the predominant energy contribution to the trend of structural changes observed for a compound series. Since TDS is a subset of structural elements of the entire S_i molecule, the number Q of s_k structural elements constituting TDS is smaller than M ($Q < M$). The summarized energy contribution, ΔE_i-(TDS), of the s_k structural elements constituting the TDS and corresponding to the S_i molecule is therefore defined as

$$\Delta E_i(\mathrm{TDS}) = \sum_1^Q \Delta e_k \qquad (3b)$$

The molecular interactions contributing to ΔE_i(TDS) are the only reason for the trend in ΔE_i. TDS has to satisfy a simple condition:

$$\Delta E_i(\mathrm{TDS})/\Delta E_i > 1 \qquad (4b)$$

(12) Bushweller, C. H.; Brown, J. H.; DiMeglio, C. M.; Gribble, G. W.; Eaton, J. T.; LeHoullier, C. S.; Olson, E. R. *J. Org. Chem.* **1995**, *60*, 268−271.

(13) (a) Forsyth, D. A.; Zhang, W.; Hanley, J. A. *J. Org. Chem.* **1996**, *61*, 1284−1289. (b) Gilchrist, J.; Duplan, J.-C.; Infarnet, Y. *Chem. Phys.* **1988**, *121*, 131−136. (c) Durrant, M. L.; Malpass, J. R. *Tetrahedron* **1995**, *51*, 7063−7076.

(14) (a) To take into account the change in geometry in the *stable conformer−NIR transition state* conformational pathway, the change of α_{av} during inversion was proposed as a good parameter.[4] The average angle α_{av} is determined as the arithmetic mean for the calculated bond angles at the N atom. (b) The averaged angle β_{av} is determined as the arithmetic mean for the calculated angles for the backbone bonds at the bridgehead C atoms. We do not consider the difference of these average angles in the NIR transition states vs the corresponding stable conformers (as it was performed, e.g., in ref 4) since this difference is similar and also very small (~0.7°) for β_{av} in these amines. In other words, the geometry (bond angles) of fragment A for stable conformers of rigid backbone amines **1a**, **2a**, and **3a** determines formally the major energy change for the itinerary *stable conformer−NIR transition state*.

(15) Brouwer, A. M.; Krijnen, B. *J. Org. Chem.* **1995**, *60*, 32−40.

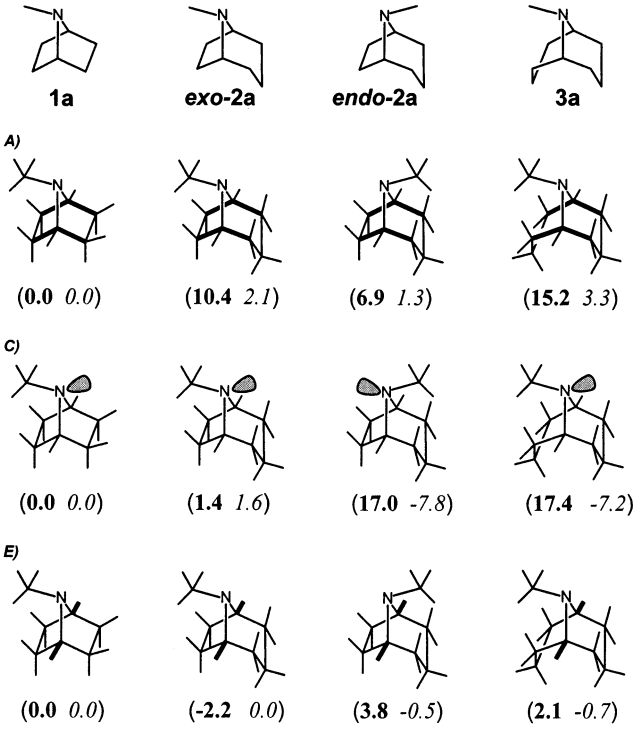

FIGURE 6. Components ΔE_i^{L}(**j**) and ΔE_i^{DA}(**j**) (in parentheses; kcal/mol) for the relative barrier decrease contributions ΔE_k(**j**) of selected fragments A, C, and E (in bold or gray) in azabicycles **1a**, **2a**, and **3a**. Values in bold represent the Lewis orbitals-related energy difference ΔE_i^{L}(**j**), while values in italics represent the NBO donor−acceptor interactions-related energy difference ΔE_i^{DA}(**j**).

satisfying both criteria. Indeed, to a smooth plot for the barrier decrease (actually a sum of all factors) corresponds a similar smooth plot (actually the fragment contribution) for fragments A + C + E (criterion i is fulfilled). The ΔE_{ACE}(**j**) values are bigger than the ΔE_k(**j**) values for individual fragments A−J. Also, other fragment combinations, for instance, A + B + C, A + C, A + B, A + E, A + G, or A + C + I, have no explicit trend, or their contribution to ΔE(**j**) is relatively small. Simply saying, the fragments A + C + E plot, if compared with the plot of the total barrier decrease ΔE(**j**), demonstrates a "concentration" in this structural fragment of a tendency to the NIR barrier decrease of amine series **1a**, **2a**, and **3a** (criterion ii is fulfilled).

Thus, in light of the NBO approach, the origin of the bicyclic effect consists mainly of the energy of the Lewis orbitals of the valent surrounding of the C_α atoms as well as of the N lone pair (see Figure 6 for the ΔE_i^{L}(**j**) and ΔE_i^{DA}(**j**) values). The energy contribution of TDS, namely, ΔE_{ACE}(**j**) = ΔE_A(**j**) + ΔE_C(**j**) + ΔE_E(**j**), is increased parallel to the decrease of the size of the rings which form the azabicyclic **j** system. Strictly speaking, the bicyclic effect should not be considered as an effect (i.e., as an exclusive attribute of a system among structurally similar systems) in the conformational dynamics of alkylamines. Unusually high NIR barriers in azanorbornanes **1** are simply a consequence of a smooth rise of this difference ΔE_{ACE}(**j**) (Figure 5) for the homologous N-bridged bicyclic amines.

Bicyclic amines with a two-atom bridge, e.g., **5a** and **6a**, in contrast to the nitrogen-bridged bicycle **1a**, possess

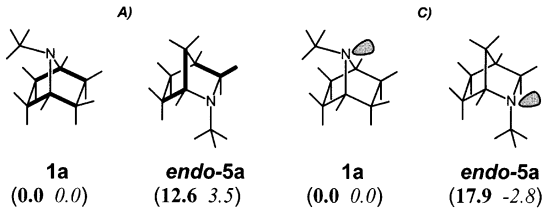

FIGURE 7. NIR rate-determining fragments A and C in the *endo*-conformer of **5a** are shown in bold/gray. The numbers in parentheses (kcal/mol) show fragmental contributions ΔE_i^{L}(**j**) (in bold) and ΔE_i^{DA}(**j**) (in italics) to the barrier decrease ΔE_k(**j**) (kcal/mol; relative to **1a**).

no high NIR barriers.[13a] For instance, there is a 6.6 kcal/mol difference between the DNMR-measured NIR barriers of azabicyclo[2.2.1]heptanes **1a**[4] and **5a**[13a] (in very good agreement, our calculations give a value of 6.3 kcal/mol; see Table 1). Also for the related azabicyclo[2.2.2]-octane **6a** the experimental barrier is low (6.6 kcal/mol[13a]). The NBO-based consideration of the A and C fragments also permits the intriguing difference in NIR barriers for the bicyclic effect systems (N-bridged bicycles **1**) and related CH_2N-bridged bicycles to be explained. The barrier decrease (for **5a** relatively to structural isomer **1a**) is caused, as for amines **1a**, **2a**, and **3a,b** above, by the difference in orbital energy ΔE_{AC}(**j**) of two C_α–C_β bonds for these compounds (i.e., fragment A; see Figure 7) as well as the nitrogen lone pair (i.e., fragment C).

2.4. Amine Structure−NIR Barrier Correlation. Earlier Approaches. Previous discussions of the origin of the bicyclic effect in azanorbornanes were mostly focused on the role of fragments B + C + D (as the N-pyramid).[4,6,12,13a−c,14a] High strain, which develops during NIR for the endocyclic CNC angle,[12] was stated to be responsible for the bicyclic effect. However, as was pointed out,[13a,b] no reliable dependence of NIR barriers on CNC angle values is actually present for cyclic amines. Supporting this criticism, our calculations give here endocyclic CNC angle values of 109.68° and 111.42° for bicycle **3a** (lower NIR barrier) and tricycle **3b** (higher NIR barrier; see Table 1), respectively. It was concluded[3a] that taking three CNC angles into consideration[14a] did not lead to a satisfactory correlation between NIR barriers and this angle parameter for different cyclic amines.

The hypothesis[13c] that the bicyclic effect in amines **1** is caused by unusual stabilization of these compounds in the stable conformation because of a delocalization of the N lone electron pair (fragment C) is not supported by the present study. The *endo*-conformer of bicycle **5a** (see Figure 1) was found by NMR to be lower in energy (by 0.3 kcal/mol) than the corresponding *exo*-conformer.[13a] Our calculation (at the MP2/6-31G* level) results are in excellent agreement with the experimental $\Delta G°$ value: the ΔE value between the *endo*- and *exo*-conformers is also 0.3 kcal/mol. Azabicycles **1a** and **5a** are structural isomers. Similar calculations, when applied comparing the stable conformer of **1a** and the lowest energy conformer of **5a** (the *endo*-conformer), showed that "the bicyclic effect system" **1a** possesses an appreciable (2.1 kcal/mol) excess of ΔE over that of the "the usual amine system" **5a**. Due to the high relevancy of our $\Delta G°$ calculations, the calculations-based result for *destabilization* of **1a** vs the isomeric *endo*-**5a** is a serious argument

for the absence of the proposed[13c] stabilization in bicycle **1a**. Furthermore, direct calculations of the occupancy of the sp^3-orbital of the nitrogen lone pair in the stable conformers of amines **1a**, **2a**, **3a,b**, **4a**, **5a**, and **6a** (within the limits of the NBO approach;[7a−c] see Table 1) show that this occupancy in azanorbornane **1a** is higher than in most other amines. Finally, the p-character of the nitrogen lone pair orbital decreases with the increase of NIR barriers for amines **1a**, **2a**, **3a,b**, **4a**, **5a**, and **6a** (Table 1). Thus, we can conclude that the higher the barrier is in these cyclic amines, the less the N lone pair participates in a π-symmetry conjugation.

Also the suggestion[13a] of the predominant role of fragments E + F due to the eclipsing of the *N*-Me group and the bridgehead H atoms in the NIR transition state for amine **1a** is not relevant. The energy for the steric interactions of these remote substituents is obviously less in the inversion transition state than in the stable conformer because of spatial divergence of the N-substituents on going from the N-pyramid to a planar nitrogen. According to our MM3-derived results for **1a** (this work), this energy difference (as steric energy difference ΔE_s) is 0.0 kcal/mol for the pair *C atom of the Me group−two bridgehead H atoms* and −0.1 kcal/mol for the pair *H atoms of the Me group−two bridgehead H atoms*.

It is now clear why previous attempts (see above) to find a correlation azacycle structure−NIR barrier were unsuccessful: only structural fragment C or E was *separately* taken into consideration, while fragment A was not even tried carefully. The possible role of the last fragment was, instead, predicted: "the C_{α}–C_{β} bonds of primary alkyl monocyclic groups are in poorer geometry for overlap than those of bicyclic alkyl groups, which might be another factor causing the bicyclic effect".[4] Our quantitative analysis shows that σ-orbitals of these bonds (i.e., of fragment A) are indeed a significant factor affecting NIR barriers in bicyclic systems (see section 2.2). Since now the fragments of the bicyclic framework were successfully arranged according to their relative significance for NIR, it was also much simpler to reveal whether a correlation between the magnitude of this barrier increase and structural parameters of nitrogen-bridged bicycles exists.

2.5. A Quantitative Azacycle Structure−NIR Barrier Correlation. The three most important structural fragments, A, C, and E, may be described in terms of molecular geometry as a combination of two C_{α}-pyramids (i.e., fragments A + E) and the N-pyramid (i.e., fragment C). Since the relative barrier height in nonfunctionalized nitrogen-bridged bicycles is determined by the combined structural fragments A + C + E, the azacycle geometry−NIR barrier relationship should be represented by taking into account a combined geometry of these three pyramids, the N-pyramid and the two C_{α}-pyramids. Indeed, the experimental NIR barriers for the stable conformers of **1a**, *exo*-**2a**, *endo*-**2a**, and **3a,b** correlate perfectly with the averaged angles α_{av} and β_{av} at the vertex of each pyramid.[14a,b] Regression analysis demonstrated that the barrier values lie close to the optimal plane (see eq 2): the standard error is 0.2 kcal/mol while $R^2 = 0.997$ at the 98% level of confidence.

$$\Delta G^{\ddagger} = -0.379\alpha_{av} - 0.753\beta_{av} + 133.8 \qquad (2)$$

No satisfactory quantitative correlation was obtained when the $C_{\alpha}NC_{\alpha}$ or $C_{\beta}C_{\alpha}C_{\beta}$ angle and α_{av} or β_{av} value were tried separately. Thus, the presence of a good correlation (eq 2) confirms our view of the unhindered[16] nitrogen-bridged bicycles as systems for which the TDS for NIR may be represented by the $C_{\alpha}-N-C_{\alpha}$ *tripyramid* backbone fragment (Figure 8).

No reliable correlation for NIR barriers of monocyclic and bicyclic amines was previously established using an α_{av}-derived parameter (see refs 3a and 4 for the discussion). Besides, four- and five-membered monoazacycles cannot be included in a set of usual inverting amines because the DNMR-measured barriers for these species are related to a concerted process of ring inversion−NIR but not to an isolated dynamic process of NIR.[5] Now we can maintain that the two-parameter correlation represented by eq 2 is suitable to correlate NIR barriers vs the structure of monocyclic (excluding three- to five-membered rings) *and* nitrogen-bridged bicyclic methylamines.[17] For instance, the experimental NIR barrier for piperidine **4b** (Figure 1) is 8.7[18a] kcal/mol. Equation 2 leads to the value 8.9 kcal/mol[18b] for the NIR barrier of this compound.

The highest known NIR barrier (13.8 kcal/mol) among the bicyclic effect systems has been measured[4] for the smallest DNMR-studied azabicycle, amine **1a**. For smaller bicycles, amines **8** and **9**, molecular mechanics calculations (by MM3) predicted high NIR barriers but were unable to estimate reliably how much higher these barriers are relative to that for **1a** (or, in previous terms, to answer whether the bicyclic effect is inherent to these amines).[1c,5a] Using the MM3-derived α_{av} and β_{av} values for **8** (108.7° and 97.5°, respectively[5a]) and for **9** (103.5° and 89.2°, respectively[1c]) in eq 2, we obtain a high value of 19.2 kcal/mol for the *endo*-conformer[18c] of azabicycle **8** and an extremely high value of 27.4 kcal/mol for azabicycle **9**. Our ab initio calculations lead to the same value of the NIR barrier (19.2 kcal/mol; this work) for amine **8**. Thus, the obtained correlation (i.e., eq 2) indeed possesses a good predictive ability. The corresponding ab

(16) Additional effects influence the NIR barrier height (for the analysis of these effects in sterically crowded amines, e.g., *N*-neopentyl or *N*-*t*-Bu derivatives, see: Nelsen, S. F.; Cunkle, G. T. *J. Org. Chem.* **1985**, *50*, 3701−3705; see also refs 3a and 10). Obviously, functionalization of the backbone may also cause specific effects on the NIR barrier in the bicyclic effect systems (see, e.g., for the ring unsaturation effects: Belkacemi, D.; Davies, J. W.; Durrant, M. L.; Walker, M. P.; Belkacemi, D.; Malpass, J. R. *Tetrahedron* **1992**, *48*, 861−884).

(17) There is no good accordance for the tetracyclic *N*-methyl-1,4-diphenyl derivative **1c** (the experimental barrier is 12.2 kcal/mol; Gribble, G. W.; Switzer, F. L.; Bushweller, J. H.; Jewett, J. G.; Brown, J. H.; Dion, J. L.; Bushweller, C. H. *J. Org. Chem.* **1996**, *61*, 4319−4327). The geometry optimization for the lowest energy conformer of **1c** at the RHF/6-31G* level (this work) provides 109.8° and 102.7° as α_{av} and β_{av} values, respectively (the corresponding MM3-derived values are 109.8° and 101.4°; see the Experimental Section for the procedure of conformational search). However, the significant deviation of the correlation-based estimate of the NIR barrier (14.8 kcal/mol) from the measured value may result from the energy contributions of orbitals of the Ph groups of azanorbornane **1c**.

(18) (a) Crabb, T. A.; Katritzky, A. R. *Adv. Hetrocycl. Chem.* **1984**, *36*, 1−176. (b) The geometry for piperidine **4b** was optimized at the MP2/6-31G* level. The C_{α}–C_{β} and C_{α}–H_{ax} bonds were taken into account for the calculation of the β_{av} value. (c) According to our ab initio calculations at the MP2/6-31G* level (this work), the *endo*-conformer of **8** is more stable than the corresponding *exo*-conformer by 4.5 kcal/mol.

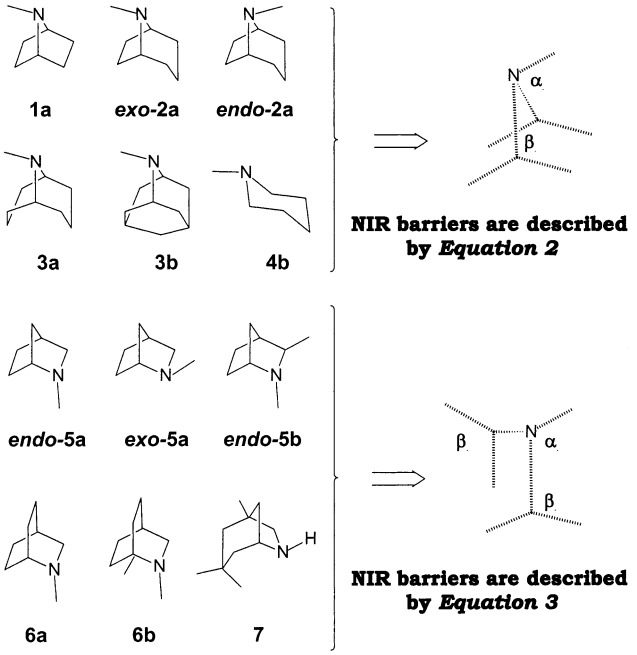

FIGURE 8. $C_\alpha-N-C_\alpha$ tripyramid backbone fragments (shown by dotted lines) which determine NIR rates for azacycles possessing different relative orientations of the C_α- and N-pyramids.

initio-based estimation of this barrier for amine **9** (24.3 kcal/mol; this work) reproduces at least the barrier range, affording a value that is the highest NIR barrier so far considered for nonfunctionalized alkylamines.

However, eq 2 for the N-bridged azabicycles **1a**, **2a**, **3a,b**, **8**, and **9** does not cover CH_2N-bridged analogues **5a** (*exo*- and *endo*-conformers) and **6a,b**. For instance, this correlation-based estimate for amine **6a** and the *endo*-conformer of **5a** gives 10.9 and 11.3 kcal/mol values, respectively, for the corresponding NIR barriers. This means that the reciprocal orientation of the N- and C_α-pyramids (i.e., a formal turn of the C_α-pyramids around their C−N edges) affects the NIR barrier and only a certain fixed arrangement of these three pyramids (see Figure 8) provides the above correlation.

Hence, the description of azacycles in terms of the $C_\alpha-N-C_\alpha$ tripyramid fragment may be valuable only if amines that possess the same relative orientation of the pyramids are compared. This assumption was tested on the example of the CH_2N-bridged azabicycles **5a** (*exo*- and *endo*-conformers), **6a,b**, and **7**. A good two-parameter correlation (the standard error is 0.3 kcal/mol and $R^2 = 0.941$ at the 98% level of confidence; eq 3)

$$\Delta G^{\ddagger} = 0.394\alpha_{av} - 0.204\beta_{av} - 15.4 \qquad (3)$$

takes place between experimental NIR barriers and calculated values α_{av} and β_{av} for these analogues (see Table 1; the NIR barrier for **7** has been determined[8c] by measuring dielectric relaxation at low temperatures). To prove this correlation, the NIR barrier for bis-α-branched amine **5b** (an analogue of bis-α-branched amines **1a**, **2a** and **3a,b**) was calculated (see Table 1). The correlation-based estimate of the barrier is only 0.9 kcal/mol lower than the calculated value. Our assumption (see above) was confirmed: NIR barriers for amino structures **5a,b** (*exo*- and *endo*-conformers), **6a,b**, and **7** possessing the $C_\alpha-N-C_\alpha$ tripyramid fragment of the same geometry correlate with the geometrical parameters of this fragment.

Thus, two *$C_\alpha-N-C_\alpha$ tripyramid geometry−NIR barrier* correlations take place for two amine sets, while the discrepancy between these sets consists of the different turn of one of the C_α-pyramids relative to the N-pyramid around their common edge (i.e., the C−N bond; see Figure 8). Consequently, a common correlation $C_\alpha-N-C_\alpha$ tripyramid geometry−NIR barrier (i.e., the correlation for cyclic or bicyclic *N*-Me amines excluding three- to five-membered monoazacycles) seems to be achievable, if a parameter which also takes into account the relative orientation of the N- and C_α-pyramids could be introduced.

The significance of this relative pyramid orientation also follows from the fact that the influence of the N lone pair is opposite for two amine series described separately by eqs 2 and 3 (the coefficients of parameter α_{av} have opposite signs). The energy of donor−acceptor interactions of the occupied orbital of the N lone pair with the vacant orbitals of the $C_\alpha-C_\beta$ bonds depends in general on the relative orientation of these structural fragments. Therefore, it may be concluded that the sign change indicates an important role of a different orientation for the C_α-pyramids relative to the N-pyramid in amines **1a**, **2a**, and **3a,b** vs amines **5a,b**, **6a,b**, and **7**.

We examined the correlation between calculated NIR barriers ($\Delta E_{calcd}^{\ddagger}$) for amines **1a**, *exo*-**2a**, *endo*-**2a**, **3a**, *endo*-**5a**, and **6a** from the above-mentioned two sets and the energy contribution of the tripyramid fragment to NIR barriers of these bicycles (i.e., the values $E_{A+E} + E_C$). A good common correlation (the standard error is 0.8 kcal/mol and $R^2 = 0.942$ at the 98% level of confidence) takes place for these azabicycles from two sets of different relative orientations of the N- and C_α-pyramids (see eq 4). The importance of this result consists of the demonstration of the possibility, in principle, of finding a relationship between structure and NIR barriers for cyclic alkylamines of different backbones.

$$\Delta E_{calcd}^{\ddagger} = 0.36\Delta E_C + 0.08\Delta E_{A+E} - 5.3 \qquad (4)$$

According to eq 4, fragments A + E contribute less to the NIR barrier correlation for these amines. Hence, in establishing the correlation azacycle geometry−NIR barrier (which is similar to the correlations expressed by eqs 2 and 3), it is possible to replace parameter β_{av} with a parameter which is sensitive mostly to the relative orientation of the N- and C_α-pyramids. Such a parameter may be less sensitive to the geometry of the C_α-pyramids.

As an adequate parameter we chose the arithmetic mean (τ_{av}) of six torsional angles $C_{NMe}-N-C_\alpha-X_\beta$ (X_β is a C_β or H_β atom).[19] Employing regression analysis with this new parameter τ_{av} as well as parameter α_{av}, a satisfactory correlation with experimental barriers was found for amino structures **1a**, *exo*-**2a**, *endo*-**2a**, **3a**, *endo*-**5a**, and **6a** (the standard error is 1.6 kcal/mol and $R^2 = 0.811$ at the 98% level of confidence; see eq 5).

(19) These dihedral angles were used for definition of the similar parameter τ_{av} establishing a qualitative relationship of *NIR barrier−N-hybridization* in amines (Andrews, P. R.; Munro, S. L. A.; Sadek, M.; Wong, M. G. *J. Chem. Soc., Perkin Trans. 2* **1988**, 711−718).

$$\Delta G^{\ddagger} = -0.737\alpha_{av} + 0.236\tau_{av} + 68.0 \qquad (5)$$

To further check the validity of this equation, we looked at bis-α-branched piperidine **4a**, piperideine **4c**, and bicyclic amine **6b**, which represent compounds with different relative orientations of the N- and C_α-pyramids. For amines **4c** and **6b** experimental NIR barriers are known (see section 2.1 and Table 1). As an NIR barrier value for amine **4a** our MM3-based calculations[10] give 9.7 kcal/mol and the present ab initio calculations (Table 1) give 10.2 kcal/mol.[20] Equation 5 provides 9.8, 9.1, and 7.4 kcal/mol for the NIR barriers for **4a**, **4c**, and **6b**, respectively. Thus, the difference between experimental values for **4c** and **6b** or the ab initio result for **4a** and the corresponding correlational estimates is 0.1, 0.8, and 0.4 kcal/mol, respectively. Nevertheless, despite the high accuracy demonstrated by the obtained generalized eq 5, two partial correlations (see eqs 2 and 3) should be considered as more reliable in the barrier estimation due to their better statistical characteristics.

Since eq 5 represents a sufficiently accurate *amine structure−NIR barrier* relationship for monocyclic (excluding three- to five-membered) and polycyclic *N*-Me/*N*-H amines, this, as well as the correlations expressed by eqs 2 and 3 for certain amine types, is a convenient tool for the NIR barrier prediction. For instance, for amines **1a**, **2a**, and **3a** we found that the correlational barrier estimations exploiting the MM3-provided α_{av} and β_{av} values do not practically differ from those estimates derived using the ab initio-optimized geometries. MM3-based geometry optimizations take usually a few seconds of computer time even for 100−200-atom molecules. An estimate of the conformational equilibrium for cyclic amines by MM3 was proven as sufficiently accurate, and therefore, identification of the lowest energy conformers by MM3 is in general reliable for azacycles.[21a] The above correlations thus may provide a simple but valuable prediction of the NIR barriers for biologically significant mono- or polycyclic alkylamino systems, i.e., alkaloids.

As an example, we present an estimate for morphine. The calculated NIR barrier for this alkaloid is 6.6 kcal/mol (by MM3; this work).[21b] Equation 2 gives a 7.3 kcal/mol value (the MM3-provided angles α_{av} and β_{av} are 113.8° and 110.8°, respectively). Thus, we can maintain that our correlation reliably predicts for morphine an NIR barrier which is unusually low for piperidine compounds (e.g., see above for the barriers of piperidines **4a**−**c**).

3. Conclusions

Reinvestigating the NIR barrier for tropane by DNMR, we found that, in contrast to the previous notion, there is no amine-unoccupied gap if the sequence of N-bridged bicycles is arranged according to the size of their NIR barriers: in this sequence tropane is placed between larger size azabicycles (pseudopelletierines) and smaller size azabicycles (azanorbornanes). Thus, the often discussed bicyclic effect is not a specific attribute of azanorbornanes alone. Considering homologous N-bridged azabicycles within the limits of the NBO approach and using sophisticated methodology for identification of the trend-determining factors (TDS; here the NIR rate-determining structural fragments), we succeeded to single out a common structural fragment (a C_{α}–N−X_{α} tripyramid) which actually determines the NIR rates for cyclic and bicyclic *N*-Me/*N*-H amines (excluding three- to five-membered monocycles). The NBO-based analysis led to the conclusion that the origin of the well-known bicyclic effect in conformational dynamics of amines originates from the different energies of σ-orbitals of C_{α}–C_{β} bonds as well as the nitrogen lone pair for different bicyclic amines. Identification of TDS permitted to analyze only its geometry and thus in a simple manner to establish good quantitative correlations for the azacycle geometry−NIR barrier. The reasons for the limitations or failures of the previous attempts to explain the bicyclic effect or to find such correlations were revealed by our results. Moreover, these correlations open the attractive possibility of transforming the prediction of the barriers for monocyclic or polycyclic amines into a routine and sufficiently accurate method.

4. Experimental Section

The commercially available tropane **2a** and the hydrochloride of **4c** (Aldrich) were used for NMR studies (**4c**·HCl was transformed into the free amine before NMR experiments). ^{1}H and ^{13}C NMR spectra were obtained on an NMR spectrometer of 600 MHz proton frequency, with TMS as internal standard. The sample (∼30 mg in 0.5 mL of CD_2Cl_2) was equilibrated for ∼10 min at each temperature before NMR acquisition. Temperatures were measured with a calibrated digital thermometer and are believed to be accurate to 0.5 K. For the complete line shape analysis a modified version of a program written by R. E. D. McClung, University of Alberta, Edmonton, Canada T6J 2G2, was used with visual fitting. The activation parameters were calculated using the Eyring equation.

Version 6.0 of the Macromodel package[22a−c] was used in the Monte Carlo-based conformational search for compound **1c** (generation of 5×10^3 structures followed by MM3*-assisted minimization with the energy upper limit 5 kcal/mol from the lowest energy conformer found). The structures of the resulting stable conformations were used as the starting geometry in the following optimizations (by MM3 or ab initio). The 1996 version of the MM3 program[23a,b] was used in molecular mechanics calculations for stable conformations and NIR transition states of the amines studied. First-order transition states of NIR in the potential energy surface generated by MM3 were located by algorithms a) and b) from ref 10. Normal-mode vibrational analysis and full-matrix minimization options of the MM3 package were employed for the energy

(20) A high NIR barrier value for **4a** (13.0 kcal/mol) was extracted from the protonation experiments in aqueous solutions (see: Delpuech, J.-J.; Deschamps, M.-N. *Nouv. J. Chim.* **1978**, *2*, 563−568). However, we cannot take into account this value due to an increase of the NIR barrier in H-bond-forming solvents as well as the serious problems in the barrier assignment (for criticism of the barrier assignment methodology see ref 5b; also see: Belostotskii, A. M.; Gottlieb, H. E.; Aped, P. *Chem.−Eur. J.* **2002**, *8*, 3016−3026).

(21) (a) Belostotskii, A. M.; Shokhen, M.; Gottlieb, H. E.; Hassner, A. *Chem.−Eur. J.* **2001**, *7*, 4715−4722. (b) For a non-H-bonded amino group in a vacuum. The MM3-based calculations for the NIR barrier of morphine were performed using algorithm a from ref 10. No correct measurement for the NIR barrier in morphine has been reported in the literature (for criticisms of the early experiments, see: Eliel, E. L.; Morris-Natschke, S.; Kolb, V. M. *Org. Magn. Reson.* **1984**, *22*, 258−262).

(22) (a) Saunders: M.; Houk, K. N.; Wu, Y. D.; Still, W. C.; Lipton, M.; Chang, G.; Guida, W. C. *J. Am. Chem. Soc.* **1990**, *112*, 1419−1427. (b) Mohamadi, F.; Richards, N. G.; Guida, W. C.; Liskamp, R.; Lipton, M.; Caufield, C.; Chang, G.; Hendrickson, T.; Still, W. C. *J. Comput. Chem.* **1990**, *11*, 440−467. (c) Macromodel, Version 6.0, Department of Chemistry, Columbia University, New York.

(23) (a) Allinger, N. L.; Yuh, Y.; Lii, J.-H. *J. Am. Chem. Soc.* **1989**,*111*, 8551−8575. (b) Schmitz, L. R.; Allinger, N. L. *J. Am. Chem. Soc.* **1990**, *112*, 8307−8315.

minimization of the transition states. The stochastic conformational search option (an MM3 package component) was used for conformational analysis of amine **5b**.

The Gaussian98 package[9] was used in ab initio calculations for the stable conformations and the NIR transition states (gas phase). *Stable conformations:* Initial ab initio geometry optimization was performed at the restricted Hartree−Fock level using the 3-21G basis set. The resulting geometry was optimized at the RHF/6-31G* level and then at the B3LYP/6-31G* or MP2/6-31G* level followed finally by calculations with the NBO option. *NIR transition states:* The same sequence in the theory level increase was employed using the Berny optimization algorithm and the Newton−Raphson optimization procedure. For the location of the first-order NIR transition states the "NoEigenTest" option was used at the initial calculation step at the 3-21G level followed by the "CalcAll" option in the next calculation step at the same level of theory. If no first-order transition state for NIR was found in calculations at the 3-21G level, only the "CalcAll" option was employed for optimization of the initial geometry or the *N*-Me group in the initial structure was rotated by 40−60° before the geometry optimization. The same sequence of Gaussian98 options was used at each level of theory, increasing the level gradually as in the calculations performed for stable conformations. Since in the case of amine **8** the above procedure sequence led at the last stage (energy minimization at the MP2/6-31G* level) only to a second-order transition state, geometry optimization for this structure was started at the MP2/6-31G* level accompanied by the calculations of the force constants at every point (the "CalcAll" option).

Acknowledgment. A Bar-Ilan University Research Grant to A.M.B. is gratefully acknowledged. We thank a group of professors from the Israeli Universities (Profs. Benjamin Fein, Eliezer Giladi, Dan Amir, Daniel Hupert, Elisha Haas, and others), the enthusiastic creators and permanent supporters of the governmental scientific KAMEA program.

JO020221I